

Prediction of the patient-specific postoperative outcome of TAVI procedure: Impact of the positioning strategy

S. Morganti^{a*}, N. Brambilla^b, F. Bedogni^b, F. Auricchio^c

^a Dip. di Ingegneria Industriale e dell'Informazione, Università degli Studi di Pavia

^b ICSA Policlinico Sant'Ambrogio, Milano

^c Dip. di Ingegneria Civile e Architettura, Università degli Studi di Pavia

Abstract

Prediction of percutaneous aortic valve replacement is of utmost importance for many reasons: Device performances and, consequently, also long-term durability are highly affected by the prosthesis positioning strategy. Medical operators look forward to a prediction of device-specific and patient-specific implantation procedure outcome which may help them choosing the optimal implantation strategy. In the present work, a patient-specific real case of CoreValve implantation has been studied: after modeling the native aortic structure including 3D calcifications from CT data, five different configurations of device implantation have been simulated changing both implantation distance and implantation angle. Quantitative measures of prosthetic valve postoperative configuration and performance are proposed. We obtain ...

1 Introduction

The first transcatheter aortic valve implantation (TAVI) dates back to 2002 [1]. Since then, many studies have demonstrated the efficacy of such a minimally-invasive approach for the treatment of severe aortic valve stenosis in critical patients [2, 3]. For patients who cannot undergo surgery, trials and registries have shown improved hemodynamics and reduced rate of death from any cause or repeat hospitalization and cardiac symptoms [4]. Even though several devices have been recently (and are going to be) introduced in the market, the two most widely implanted valves are the balloon-expandable Edwards SAPIEN and the self-expandable Medtronic Corevalve, which have shown similar (good) short- and (poor) long-term outcomes [5]. Durability, in fact, still represents one of the most critical aspect of TAVI devices [6], especially in the future perspective of extending such a minimally-invasive approach to younger, lower-risk patients who suffer from surgical/technical risk factors for open chest surgery [7].

It has been shown that geometric factors can be responsible of reduced device durability [8]: stent deformation, in particular, can affect leaflet coaptation and induce higher asymmetrical stresses both on the prosthetic leaflets and on the stent [9, 10]. The placement strategy and the choice of the device landing zone have significant impact on the postoperative stent

*Corresponding author. Email: simone.morganti@unipv.it

configuration and deformation, and, consequently, on the global valve postoperative performance.

In particular, it has been proven that the valve implantation depth represents a factor associated with cardiac conduction disorders and permanent pacemaker implantation [11, 12]. Fraccaro et al. (2011) [13] confirmed what is also expected: The deeper the prosthetic device is implanted, the greater the risk of compression of the left bundle branch, leading to an increased occurrence of cardiac disorders. Not only the placement depth, but also the stent implantation angle, measured between the left ventricular outflow tract and the ascending aorta, has shown to have great impact on prosthesis performance, and in particular on paravalvular regurgitation [14]. Moreover, the presence of calcifications can considerably affect prosthesis implantation leading to a non-uniform expansion of the stent frames at all levels, thus inducing stent deformation and consequent poor TAVI procedure outcome [15]. Current understanding of the potential adverse events associated with the TAVI procedure is still limited [16]. Certainly, many complications may arise in case of non-optimal choice of prosthetic device and implantation strategy for a specific pathological situation. A better understanding of the potential complications associated with TAVI through the prediction of what-if scenarios can help improve the procedure outcomes, allowing a wider and safer application of this surgical treatment.

All these considerations highlight a strong need of a guided (personalized) selection and sizing of the prosthetic device and implantation strategy, as also pointed out by [5]. In this context, finite element analysis (FEA) represents a consolidated mathematical tool able to provide reliable predictions of the post-implant device configuration, thus leading to the pre-operative optimal selection of the specific prosthesis (in terms of both type and size) tailored for the specific patient.

Due to its capability in handling also very complex problems (involving large deformations, contact, geometrical and material non-linearities), FEA has been already considered as a valuable numerical technique to virtually reproduce TAVI. Very recently, FEA has been used to simulate percutaneous valve implantation of balloon-expandable devices in real clinical cases [17, 18]. Self-expandable devices, and, in particular, the Medtronic Corevalve prosthesis has been investigated by Hopf et al. (2014) [19] with the aim of reconstructing the forces induced by the stent on the aortic valve complex, and by Gessat et al. (2014) [20] who proposed an image-based system to evaluate the interface forces between the Nitinol stent and the surrounding tissues. The radial forces of the Corevalve have been also evaluated by Tzamtzis et al. (2013) [21] who addressed a comparison with the Edwards SAPIEN device.

In this work, following the explicit needs of medical operators performing the TAVI procedure, we focus only on a single clinical case of Corevalve implantation with the aim of using FEA to investigate the effects of different placement choices on the final configuration of the implanted stent. In the present study, the native aortic valve and the calcifications are extracted from CT images and included in our finite element model, while the prosthetic device has been scanned with a microCT machine, thus allowing very realistic simulation outcomes. The goal is then to understand and quantitatively evaluate the effects of the stent implantation angle and depth in terms of post-implant asymmetries, stress/strain patterns, paravalvular leakage, and valve coaptation.

2 Materials and Methods

2.1 Simulation framework

The framework followed to set-up the stent expansion analysis is based on the work by [17]. ITK-Snap v.2.4 is used to extract the STL representation of the aortic root and calcific deposits [22] from CT images of a 75 year-old male patient. An in-house code is used to process the STL file and generate the finite element mesh of the aortic root (modeled with tetrahedral elements) including the native leaflets (modeled with shell elements assuming a uniform thickness of 0.5 mm [23]). The lines of leaflet attachment and the leaflet free-margin lengths are taken from the CT 3D reconstruction and from short-axis ultrasound images, respectively. The smaller calcific spots and especially those extracted at the ascending aorta level are removed; Only larger blocks of calcium at the aortic root level are thus considered. The STL file of calcifications is then processed using VMTK (Vascular Modeling ToolKit) to extract a regular tetrahedral mesh [24]. Given the comparative nature of the present study focused on the prosthetic device post-operative configuration and performance, simplified linear elastic properties are adopted to model the aortic tissue, the native leaflets, and calcifications. In particular, for the aortic root a Young modulus E of 2 MPa, a Poisson's ratio ν of 0.45, and a density ρ of 2000 kgm^{-3} is used; for the native leaflets $E = 8 \text{ MPa}$, $\nu = 0.45$, and $\rho = 1100 \text{ kgm}^{-3}$ are considered [25] while for the calcifications $E = 10 \text{ MPa}$, $\nu = 0.35$, and $\rho = 2000 \text{ kgm}^{-3}$ are used [17]. In Figure 1 a synthetic sketch summarizes the developed workflow.

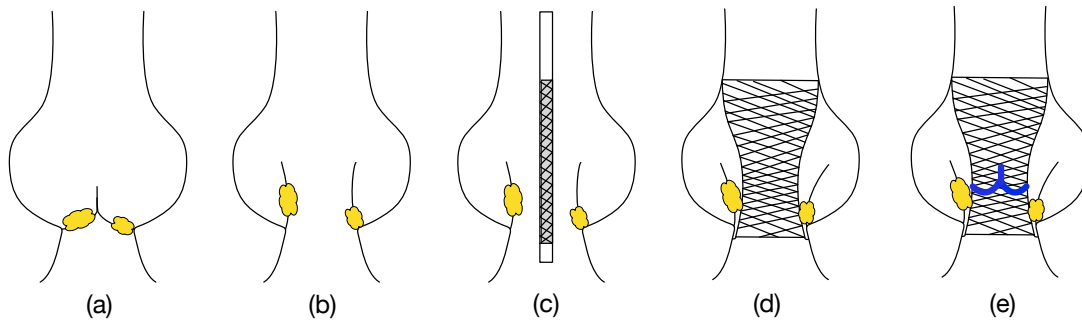


Figure 1: Sketch of simulation framework. (a) Native aortic valve model reconstructed in the diastolic phase from CT images and ultrasound measures; (b) native valve opening; (c) CoreValve stent crimping; (d) CoreValve stent expansion; (e) Prosthetic leaflets mapping inside the stent and closure.

The model of the aortic valve with calcifications is reconstructed from images recorded in the diastolic phase (Figure 1a). A pre-simulation of leaflet opening is thus performed before stent implantation (Figure 1b). Abaqus Explicit solver (3DS, Dassault Systèmes, Paris, France) is used for all the simulations presented in our study. A kinematic constraint is defined to couple the motion of the calcific deposits on the leaflets and the leaflets themselves. The CoreValve model size 29 is generated from a micro-CT scan of the actual device that allows a very accurate geometrical reconstruction. A shape-memory alloy constitutive model able to reproduce the super-elastic effect is used. Nitinol properties are assigned to the hexahedral elements of the stent mesh according to [26].

The simulation of prosthesis implantation is performed in two steps: first, as sketched in Figure 1c, the device is crimped within a rigid cylinder modeled with surface elements

to a diameter of 6 mm (18F), then the rigid catheter is gradually removed with a sliding upwards movement to let the stent expand exploiting the Nitinol super-elastic effect (Figure 1d). In the first step, frictionless contact is enabled only between the catheter and the stent, while, in the second step, contact is defined also between the stent and the aortic valve and calcifications. Finally, following [26], the prosthetic valve is mapped inside the implanted stent and a physiologic pressure is applied to the leaflets to reproduce the diastolic behavior (Figure 1e).

The simulation strategy described above has been implemented and repeatedly used to evaluate the impact of different positioning choices on prosthesis post-operative configuration and performance. In particular, three different implantation depths and angles are analyzed, as summarized in Figure 2.

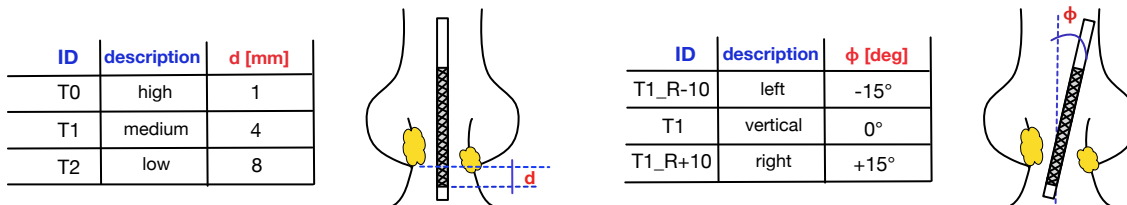


Figure 2: Summary of the simulated device configurations within the patient’s aortic valve model.

2.2 Simulation postprocessing

Each simulated configuration has been post-processed to extract quantitative measures of: (i) prosthetic stent deformation, (ii) grade of device apposition, (iii) prosthetic valve performance. In particular, stent deformation is evaluated by measuring the eccentricity of the device cross-section. In Figure 3 an example of eccentricity measurement is reported for the configuration named T2 (see Figure 2): On the left, three representative cross-sections (at the bottom, middle, and top of the stent) are shown. The nodes of the stent corresponding to the specific cross-section are extracted (red dots in Figure 3a) and used to fit an ellipse (blue line) from which the minor (a) and major (b) axes are highlighted. The eccentricity is evaluated as the ratio between the two axes: $e = b/a$. As an example, the curve representing the eccentricity along the device height is shown in Figure 3b.

The grade of device apposition and, consequently, a correspondent measure of device anchoring can be evaluated by measuring the area of the contact surface between the stent and the aortic root (called *stent-root interaction area*). In particular, we consider only the elements of the aortic root whose contact pressure after stent expansion simulation is greater than 0 and, then, we sum the areas of all the considered element faces belonging to the internal surface of the root. Such a “contact” measure also represents the grade of stent apposition and device anchoring.

The risk of paravalvular leakage can be associated to the mismatch (i.e., missed adhesion) between the implanted Corevalve stent, on one side, and the aortic valve structure (including calcifications), on the other side. Following the strategy proposed in [17], the index of potential paravalvular leakage is related to the total area of such a mismatch generating paravalvular holes (highlighted by a red line in Figure 4) measured taking a cross-section of the whole model in the plane through the three end-points of the prosthetic leaflets attachment lines

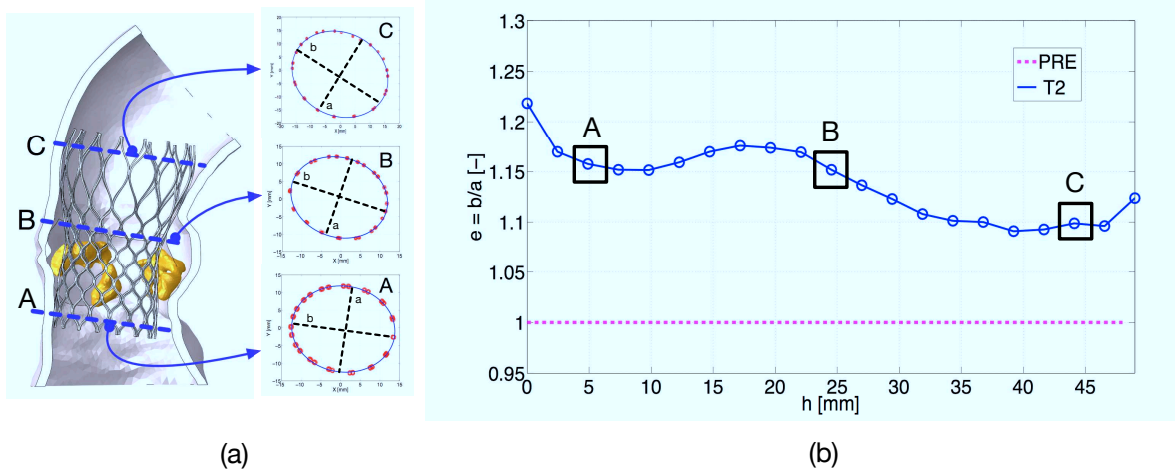


Figure 3: Postprocessing of simulation outcomes: measure of post-implant stent eccentricity. (a) three representative cross sections of the implanted device are shown; (b) the obtained eccentricity is plotted for 21 equally-spaced stent sections.

(see again Figure 4 as example).

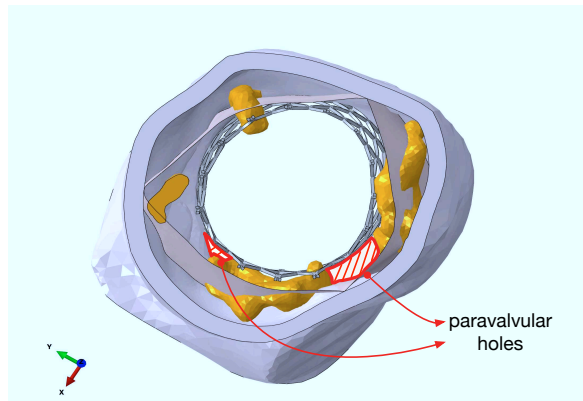


Figure 4: Paravalvular holes are highlighted from the simulation outcome of stent implantation.

Finally, the coaptation area, measured as the total area of the leaflet elements in contact each other, and the average von Mises stress on the leaflets obtained from Equation 4 reported in [27] are computed to evaluate prosthetic leaflet performance.

3 Results

The aim of the present work is to evaluate the impact of positioning on the post-operative configuration and performance of the prosthetic device used for percutaneous aortic valve replacement. FEA is used to achieve the goal starting from medical images of a real case. In this section, the obtained results are presented in terms of:

- prosthetic stent deformation: In particular, measurements of the elliptic shape of the implanted device are used to evaluate stent deformation. In Fig. 5(a) the eccentricity

(measured as described in Section 2.2) is plotted versus the stent height for configurations T0, T1, and T2 highlighting the impact of the positioning depth d , and in Figure 5(b) for configurations T1, T1_R-10, and T1_R+10, highlighting the impact of the positioning angle Φ . The maximum distortion ($e = 1.32$) is obtained for the T1_R-10 configuration.

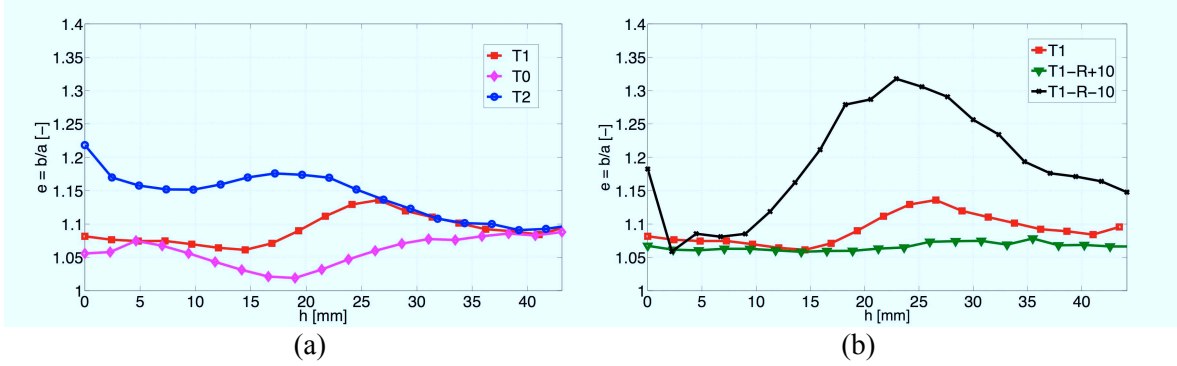


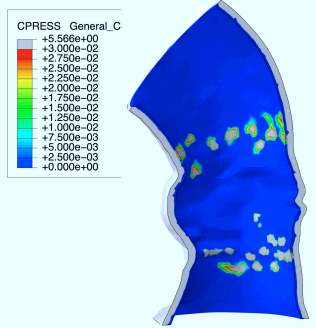
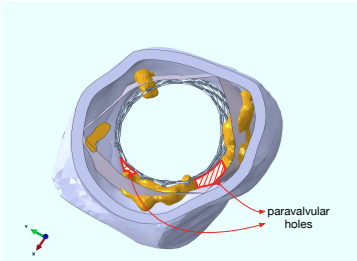
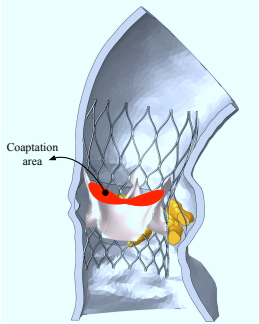
Figure 5: Measure of stent cross-section eccentricity for each simulated configuration.

- grade of device apposition: the total area of the internal root surface involved in the contact with the stent is measured for each simulated configuration and reported in Table 1.
- measure of paravalvular leakage: In particular, the grade of mismatch between the expanded stent and the internal aortic root surface is measured in the plane passing through the three commissural points of the prosthetic valve. The obtained values are reported for each configuration in Table 1.
- measure of coaptation area: the area of the elements of the three prosthetic leaflets in contact each other after valve closure simulation is measured and reported in Table 1.

4 Discussion

5 Acknowledgements

Table 1: The main quantitative results of prosthesis performance are resumed for each simulated configuration.

Stent-root interaction area	Configuration	[mm ²]
	T0	131.1
	T1	222.8
	T2	130.9
	T1_R+10	168.1
	T1_R-10	166.1
Paravalvular holes	Configuration	[mm ²]
	T0	6.8
	T1	12.9
	T2	18.6
	T1_R+10	5.3
	T1_R-10	8.7
Coaptation area	Configuration	[mm ²]
	T0	91.6
	T1	91.5
	T2	54.8
	T1_R+10	89.8
	T1_R-10	60.3

References

- [1] A. Cribier, H. Eltchaninoff, A. Bash, N. Borenstein, C. Tron, F. Bauer, G. Derumeaux, F. Anselme, F. Laborde, and M.B. Leon. Percutaneous transcatheter implantation of an aortic valve prosthesis for calcific aortic stenosis: First human case description. *Circulation*, 106:3006–3008, 2002.
- [2] C. R. Smith et al. Transcatheter versus surgical aortic-valve replacement in high-risk patients. *The New England Journal of Medicine*, 364:2187–2198, 2011.
- [3] M. Gilard et al. Registry of transcatheter aortic-valve implantation in high-risk patients. *New England Journal of Medicine*, 366:1705–1715, 2012.
- [4] M. B. Leon, C. R. Smith, M. Mack, D. C. Miller, J. W. Moses, L. G. Svensson, E. M. Tuzcu, and J. G. Webb et al. Transcatheter aortic-valve implantation for aortic stenosis in patients who cannot undergo surgery. *New England Journal of Medicine*, 363(17):1597–1607, 2010.
- [5] J. Iqbal and P. W. Serruys. Comparison of Medtronic CoreValve and Edwards Sapien XT for transcatheter aortic valve implantation. *JACC: Cardiovascular Interventions*, 7:293–295, 2014.
- [6] A. Vahanian, O. Alfieri, N. Al-Attar, M. Antunes, J. Bax, and B. Cormier et al. Transcatheter valve implantation for patients with aortic stenosis: a position statement from the European Association of Cardio-Thoracic Surgery (EACTS) and the European Society of Cardiology (ESC), in collaboration with the European Association of Percutaneous Cardiovascular Interventions (EAPCI). *European Heart Journal*, 29:1463–1470, 2008.
- [7] O. Wendler and R. Dworakowski. Tavi in patients unsuitable for surgery: A prognostic benefit for all? *Journal of the American College of Cardiology*, 63:912–913, 2014.
- [8] C. J. Schultz, A. Weustink, N. Piazza, A. Otten, N. Mollet, G. Krestin, R. J. van Geuns, P. de Feyter, P.W.J. Serruys, and P. de Jaegere. Geometry and degree of apposition of the CoreValve ReValving system with multislice computed tomography after implantation in patients with aortic stenosis. *Journal of the American College of Cardiology*, 54:911–918, 2009.
- [9] R. Zegdi, V. Ciobotaru, M. Noghin, G. Sleilaty, A. Lafont, C. Latrémouille, A. Deloche, and J.-N. Fabiani. Is it reasonable to treat all calcified stenotic aortic valves with a valved stent? *Journal of the American College of Cardiology*, 51:579–584, 2008.
- [10] M. Thubrikar, S.P. Nolan, L.P. Boshier, and J.D. Deck. The cyclic changes and structure of the base of the aortic valve. *American Heart Journal*, 99:217–224, 1980.
- [11] J. Baan, Z.Y. Yong, K.T. Koch, J.P.S. Henriques, B.J. Bouma, M.M. Vis, R. Cocchieri, J.J. Piek, and B. de Mol. Factors associated with cardiac conduction disorders and permanent pacemaker implantation after percutaneous aortic valve implantation with the CoreValve prosthesis. *American Heart Journal*, 159:497–503, 2009.
- [12] L. Roten, P. Wenaweser, E. Delecrétaz, G. Hellige, S. Stortecky, H. Tanner, T. Pilgrim, A. Kadner, Eberle, M. Zwahlen, T. Carrel, B. Meier, and S. Windecker. Incidence and

- predictors of atrioventricular conduction impairment after transcatheter aortic valve implantation. *American Journal of Cardiology*, 106:1472–1480, 2010.
- [13] C. Fraccaro, G. Buja, G. Tarantini, V. Gasparetto, L. Leoni, R. Razzolini, D. Corrado, R. Bonato, C. Basso, G. Thiene, G. Gerosa, G. Isabella, S. Iliceto, and M. Napolitano. Incidence, predictors, and outcome of conduction disorders after transcatheter self-expandable aortic valve implantation. *The American Journal of Cardiology*, doi:10.1016/j.amjcard.2010.10.054, 2010.
- [14] M. A. Sherif, M. Abdel-Wahab, B. Stöcker, V. Geist, D. Richardt, R. Tölg, and G. Richardt. Anatomic and procedural predictors of paravalvular aortic regurgitation after implantation of the Medtronic CoreValve bioprosthesis. *Journal of the American College of Cardiology*, 56:1623–9, 2010.
- [15] D. John, L. Buellesfeld, S. Yuecel, R. Mueller, G. Latsios, H. Beucher, U. Gerckens, and E. Grube. Correlation of device landing zone calcification and acute procedural success in patients undergoing transcatheter aortic valve implantations with the self-expanding CoreValve prosthesis. *JACC: Cardiovascular Interventions*, 3:233–243, 2010.
- [16] J.B. Masson, J. Kovac, G. Schuler, J. Ye, A. Cheung, S. Kapadia, M.E. Tuzcu, S. Kodali, Martin B. M.B. Leon, and J.G. Webb. Transcatheter aortic valve implantation review of the nature, management, and avoidance of procedural complications. *JACC: Cardiovascular Interventions*, 2(9):811–820, 2009.
- [17] S. Morganti, M. Conti, M. Aiello, A. Valentini, A. Mazzola, A. Reali, and F. Auricchio. Simulation of transcatheter aortic valve implantation through patient-specific finite element analysis: Two clinical cases. *Journal of Biomechanics*, 47:2547–2555, 2014.
- [18] F. Auricchio, M. Conti, S. Morganti, and A. Reali. Simulation of transcatheter aortic valve implantation: a patient-specific finite element approach. *Computer Methods in Biomechanics and Biomedical Engineering*, page <http://dx.doi.org/10.1080/10255842.2012.746676>, 2013.
- [19] R. Hopf, M. Gessat, V. Falk, and E. Mazza. Reconstruction of stent induced loading forces on the aortic valve complex. In *MICCAI-STENT 2012, 1st MICCAI Workshop on Computer Assisted Stenting*, 2012.
- [20] M. Gessat, R. Hopf, T. Pollok, C. Russ, T. Frauenfelder, S.H. Sündermann, S. Hirsch, E. Mazza, G. Székely, and V. Falk. Image-based mechanical analysis of stent deformation: Concept and exemplary implementation for aortic valve stents. *IEEE TRANSACTIONS ON BIOMEDICAL ENGINEERING*, 61:4–15, 2014.
- [21] S. Tzamtzis, J. Viquerat, J. Yapc, M.J. Mullenc, and G. Burriesci. Numerical analysis of the radial force produced by the medtronic-corevalve and edwards-sapien after transcatheter aortic valve implantation (tavi). *Medical Engineering & Physics*, 35(0):125–130, 2013.
- [22] P.A. Yushkevich, J. Piven, H.C. Hazlett, R.G. Smith, S. Ho, J.C. Gee, and G. Gerig. User-guided 3D active contour segmentation of anatomical structures: Significantly improved efficiency and reliability. *Neuroimage*, 31(3):1116:1128, 2006.

- [23] F. Auricchio, M. Conti, S. Morganti, and A. Reali. Simulation of transcatheter aortic valve implantation: a patient-specific finite element approach. *Computer Methods in Biomechanics and Biomedical Engineering*, accepted for Publication:–, 2012.
- [24] L. Antiga, M. Piccinelli, L. Botti, B. Ene-Iordache, A. Remuzzi, and D.A. Steinman. An image-based modeling framework for patient-specific computational hemodynamics. *Medical and Biological Engineering and Computing*, 46:1097–1112, 2008.
- [25] F.L. Xiong, W.A. Goetz, C.K. Chong, Y.L. Chua, S. Pfeifer, E. Wintermantel, and J.H. Yeo. Finite element investigation of stentless pericardial aortic valves: Relevance of leaflet geometry. *Annals of Biomedical Engineering*, 38:1908–1918, 2010.
- [26] F. Auricchio, M. Conti, S. Morganti, and A. Reali. Shape-memory alloys: from constitutive modeling to finite element analysis of stent deployment. *Computer Modeling in Engineering and Sciences*, 57:225–243, 2010.
- [27] F. Auricchio, M. Conti, S. Morganti, and P. Totaro. A computational tool to support pre-operative planning of stentless aortic valve implant. *Medical Engineering & Physics*, 33(10):1183 – 1192, 2011.